Available online at www.sciencedirect.com
SCIENCE DIRECT®
PERGAMON
Polyhedron 22 (2003) 45–51
POLYHEDRON
www.elsevier.com/locate/poly

Characterization of $[Fe(AMN_3S_3sarH)]^{3+}$ —a rigorously low-spin iron(II) complex

Clint A. Sharrad, Lawrence R. Gahan *

Department of Chemistry, The University of Queensland, Brisbane, Qld. 4072, Australia

Received 24 June 2002; accepted 9 September 2002

Abstract

The iron(II) complex $[Fe(AMN_3S_3sarH)](ClO_4)_3 \cdot 3H_2O$ (AMN_3S_3sarH = 8-ammonio-1-methyl-3,13,16-trithia-6,10,19-triazabicyclo[6.6.6]icosane) has been synthesized and characterized by single crystal structure and spectroscopic methods. The Fe(II)–S(thiaether) bond lengths are short, indicative of a large degree of metal–ligand orbital mixing (π-acceptor character) of the thiaether ligand. The complex is stable to metal centred oxidation.
© 2002 Elsevier Science Ltd. All rights reserved.

Keywords: Encapsulating ligand; Iron(II); Low-spin; π-Acceptor; Thiaether

1. Introduction

Six coordinate iron(II) complexes are known to exhibit sophisticated magnetic behavior [1]. For example, the iron(II) complex $[Fe(ptz)_6](BF_4)_2$ (ptz = 1-propyltetrazole) exhibits a light induced low-spin to high-spin conversion below 50 K [2], and there are numerous other examples of spin crossover systems [1]. There are examples where the magnetic behavior exhibits a pronounced anion dependence, for example for the complex $[Fe([9]aneN_3)_2]^{2+}$ ([9]aneN$_3$ = 1,4,7-triazacyclononane) the dibromide tetrahydrate is diamagnetic, but removal of the water of crystallization yields a paramagnetic material [3]. Moderation of the chromophore can also influence the spin state. Thus, the iron(II) complex $[Fe([9]aneN_2S)]^{2+}$ ([9]aneN$_2$S = 1-thia-4,7-dithiacyclononane) exhibits a temperature dependent magnetic moment (2–300 K) [4]. Incorporation of more thiaether donors results in low-spin behavior, exemplified by the N_2S_4 and S_6 complexes $[Fe([9]aneNS_2)_2]^{2+}$ ([9]aneNS$_2$ = 1,4-dithia-7-azacyclononane) [4] and $[Fe([9]aneS_3)_2]^{2+}$ ([9]aneS$_3$ = 1,4,7-trithiacyclononane) [3]. In the case of the iron(II) complexes of encapsulating N_6sar type ligands (sar = 3,6,10,13,16,19-hexaazabicyclo[6.6.6]icosane) the high-spin or low-spin d^6 condition is dependent on the apical substituents on the encapsulating ligand [5–7]. Thus, the $[Fe((NH_3)_2sar)]Cl_2Br_2 \cdot 4H_2O$ and $[Fe(sar)](CF_3SO_3)_2$ complexes exhibit high-spin behavior whereas the $[Fe((NH_2)_2sar)](CF_3SO_3)_2$ complex exhibits low-spin properties. Protonation of both primary amine sites of $[Fe((NH_2)_2sar)]^{2+}$ seemingly causes a spin crossover from high-spin to low-spin [5–7].

In an effort to further explore the magnetic behavior of iron(II) complexes we have sought to combine the known effects of the variation in chromophore and protonation state. We have thus focussed on the complex $[Fe(AMN_3S_3sarH)]^{3+}$ (AMN_3S_3sarH = 8-ammonio-1-methyl-3,13,16-trithia-6,10,19-triazabicyclo[6.6.6]icosane), an iron(II) complex with the N_3S_3 chromophore [8]. Comparisons are made with the spectroscopic properties of a number of low-spin iron(II) complexes.

* Corresponding author. Tel.: +61-733-65-3844; fax: +61-733-65-4299
E-mail address: gahan@mailbox.uq.edu.au (L.R. Gahan).

0277-5387/02/$ - see front matter © 2002 Elsevier Science Ltd. All rights reserved.
PII: S0277-5387(02)01259-7

2. Experimental

2.1. Methods

^{13}C (^{1}H decoupled), ^{13}C DEPT and ^{1}H NMR were recorded with a Bruker AC200F 200 MHz or a Bruker 400 MHz spectrometer. Variable temperature ^{1}H NMR spectra were recorded with a Bruker AC200F 200 MHz spectrometer. D_2O was employed as solvent with either 1,4-dioxane (^{13}C δ 0 ppm) or sodium 2,2-dimethyl-2-silapentane-5-sulfonate (^{1}H δ 0 ppm) used as the internal reference.

UV–Vis spectra were recorded with a Perkin–Elmer Lambda 40 spectrometer. Nafion films (Aldrich Nafion 117 perflourinated membrane 0.0007 in. thick) of the metal complexes as the perchlorate salt were prepared by placing the film in a dimethylformamide solution of the complex for 48 h. The films were removed from the solution and dried on tissue paper. In order to observe weakly absorbing bands several films were stacked on one another. UV–Vis spectra of these films were recorded with a Cary 17 spectrophotometer at room temperature (r.t.) and at $\sim$14 K, the low temperature spectra were obtained using a Leybold Heyaeus ROK 10–300 closed cycle helium cryostat system.

Cyclic voltammograms were recorded with a BAS100B/W electrochemical analyzer with a standard three-electrode system. The working electrode was glassy carbon with a platinum auxiliary electrode. The reference electrode was a Ag/AgCl (saturated $NaClO_4$, +231 mV vs. SHE). The salt bridge was filled with an inert electrolyte concentration of 0.1 M Et_4NClO_4 for both water and acetonitrile solutions employed in the working compartment. The effect of pH was studied for the water solution by adjusting the H^+ concentration with solutions of Et_4NOH and $HClO_4$. The electrode surfaces were cleaned with alumina prior to, and between, measurements. Data were recorded at 25 °C after the solutions had been degassed with nitrogen. A scan rate of 50 mV s^{-1} was employed for all measurements.

Low-resolution ESI mass spectra were obtained using a Finnigan MAT 900 XL mass spectrometer and methanol–water (40:60) solutions of the metal complexes. Spectra were recorded varying the capillary and skimmer potentials (50–200 V) so as to optimize the intensity of the signals obtained.

2.2. Preparations

The ligand AMN_3S_3sar was synthesized as described previously [8].

Caution! Although the perchlorate salt described in this work does not appear to be sensitive to shock or heat, this material like all perchlorates should be treated with caution.

2.2.1. $[Fe(AMN_3S_3sarH)](ClO_4)_3\cdot 3H_2O$

To a nitrogen purged methanol solution (25 cm^3) of AMN_3S_3sar (1.0 g) a methanol solution (25 cm^3) of ferrous perchlorate (1.0 g) was added, drop wise with stirring. The solution was stirred and the stream of nitrogen maintained for 1 h at r.t. after the completion of the addition. The solution was permitted to stand and the purple product obtained was dissolved in water (60 cm^3). The solution was filtered and to the filtrate was added several drops of concentrated $HClO_4$ (pH < 2). Upon standing for several days dark purple crystals of $[Fe(AMN_3S_3sarH)](ClO_4)_3\cdot 3H_2O$ (1.9 g, 89%) formed. (Found: C, 23.5; H, 4.97; N, 7.5. $C_{15}H_{39}Cl_3FeN_4O_{15}S_3$ requires C, 23.3; H, 5.08; N, 7.2%). Visible spectrum [λ nm (ε, M^{-1} cm^{-1}) in H_2O]: (pH 2.2) 404 (180), 559 (210); (pH 10.9) 404 (160), 559 (190). ^{13}C NMR (D_2O), δ_C: −37.4 (CH_3); −29.5 (CH_3–C_q); −27.9, −27.5 (CH_2–S–); −12.8 (N–C_q); −11.8, −8.7 (NH–CH_2).

2.3. Crystallography

2.3.1. Crystal data and refinement details

For diffractometry the purple crystal was mounted on a glass fibre with Supa glue. Lattice parameters at 293(2) K were determined by least-squares fits to the setting parameters of 25 independent reflections, measured and refined on an Enraf–Nonius CAD4 diffractometer using graphite-monochromated Mo Kα radiation employing the θ scan technique. A total of 5185 independent reflections were recorded in the range of $2.02^\circ < \theta < 24.98^\circ$. The structure was solved by direct methods. Programs used were SHELXS [9], and SHELXL-93 [10] for solution and refinement, respectively, and ORTEP [11] for plotting. Hydrogen atoms were included at calculated sites with fixed isotropic parameters. Crystal data and structure determination details are given in Table 1. The geometry of the molecule is shown in Fig. 1 together with the atomic numbering scheme. Selected bond lengths and bond angles are given in Table 2.

2.4. Potentiometric titrations and data evaluation

The potentiometric titration was carried out under a nitrogen atmosphere of nitrogen saturated water in a water-jacketed vessel maintained at 298.0 K. Data were obtained from 10 cm^3 aliquots of solutions containing 0.006 M $HClO_4$, 0.10 M Et_4NClO_4 and approximately 1.0×10^{-3} mol of ligand titrated with 0.10 M Et_4NOH. A Metrohm E665 Dosimat autoburette equipped with a 5 cm^3 burette was used to deliver the titrant and the potential measured with an Orion Ross Sure Flow 81-72BN combination electrode containing 0.1 M Et_4NClO_4 in water as the filling solution and connected to an

Table 1
Crystal data and structure refinement for [Fe(AMN_3S_3sarH)]$(ClO_4)_3 \cdot 3H_2O$

Empirical formula	$C_{15}H_{39}Cl_3FeN_4O_{15}S_3$
Formula weight	773.88
Temperature (K)	293(2)
Crystal system	monoclinic
Crystal dimensions (mm)	$0.6 \times 0.5 \times 0.15$
Space group	$P2_1/n$
a (Å)	18.724(4)
b (Å)	9.1458(5)
c (Å)	19.172(3)
β (°)	115.753(7)
V (Å^3)	2957.0(8)
Z	4
D_{calc} (g cm^{-3})	1.738
Absorption coefficient (mm^{-1})	1.066
$F(000)$	1608
θ min, θ max (°)	2.02–24.98
Limiting indices	$0 \le h \le 22, 0 \le k \le 10, -22 \le l \le 20$
Independent reflections	5185 [$R_{int} = 0.0598$]
Observed reflections	4125
Refinement method	full-matrix least-squares on F^2
Data/restraints/parameters	5185/0/370
S	0.931
[$I > 2\sigma(I)$]	$R_1 = 0.0492$, $wR_2 = 0.1379$
Largest peak and hole (Å^{-3})	1.019 and −0.703

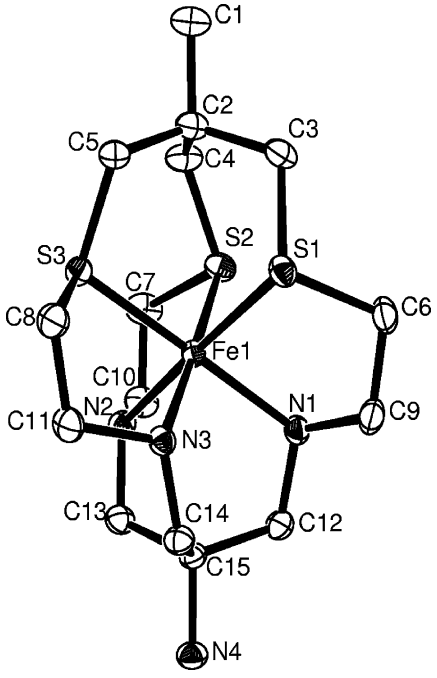

Fig. 1. ORTEP view of the structure of the complex cation [Fe(AMN_3S_3sarH)]$^{3+}$.

Orion 720A pH meter. The autoburette and pH meter were connected to an IBM compatible personal computer which controlled the addition of titrant using a locally written program so that successive additions of titrant caused a decrease of 4 mV in the potential reading. The electrode was calibrated by a strong base to strong acid titration in the absence of ligand and fitting the resulting data to the Nernst equation. The pK_a was determined using the program SUPERQUAD [12].

Table 2
Selected bond lengths (Å) and angles (°) for [Fe(AMN_3S_3sarH)]$(ClO_4)_3 \cdot 3H_2O$

Bond lengths			
Fe(1)–N(1)	2.049(3)	Fe(1)–N(2)	2.033(3)
Fe(1)–N(3)	2.048(3)	Fe(1)–S(1)	2.228(1)
Fe(1)–S(2)	2.226(1)	Fe(1)–S(3)	2.219(1)
Bond angles			
N(1)–Fe(1)–N(2)	90.25(12)	N(1)–Fe(1)–N(3)	90.13(12)
N(1)–Fe(1)–S(1)	87.50(9)	N(1)–Fe(1)–S(2)	90.96(9)
N(1)–Fe(1)–S(3)	177.29(9)	N(2)–Fe(1)–N(3)	90.48(12)
N(2)–Fe(1)–S(1)	177.17(10)	N(2)–Fe(1)–S(2)	87.35(9)
N(2)–Fe(1)–S(3)	90.62(9)	N(3)–Fe(1)–S(1)	91.24(9)
N(3)–Fe(1)–S(2)	177.58(9)	N(3)–Fe(1)–S(3)	87.30(9)
S(1)–Fe(1)–S(2)	91.97(4)	S(1)–Fe(1)–S(3)	91.70(4)
S(2)–Fe(1)–S(3)	91.64(4)		

3. Results and discussion

Reaction of AMN_3S_3sar, an encapsulating ligand containing secondary amine and thiaether donors, with an iron(II) salt in methanol under an atmosphere of dinitrogen results in a purple solid which can be crystallized from acid solution as purple blocks. The product, characterized as the iron(II) complex [Fe(AMN_3S_3sarH)]$(ClO_4)_3 \cdot 3H_2O$, is stable to oxidation in the solid state and in aqueous solution unlike the $[Fe(sar)]^{2+}$ and $[Fe((NH_3)_2sar)]^{4+}$ analogues which oxidize readily to give imines [5–7] resulting in an intense absorbance in the UV–Vis at around 22 000 cm^{-1}. The cyclic voltammogram of an aqueous solution of the iron(II) complex suggested that the complex did not undergo metal centered redox chemistry in the potential range (−1000 to +600 mV vs. Ag/AgCl) investigated. Attempts to prepare the iron(III) complex of AMN_3S_3sar by reaction of the free ligand and iron(III) resulted in a mixture of products.

The ^{13}C NMR spectrum of [Fe(AMN_3S_3sarH)]$^{3+}$ exhibits a seven line pattern. Based on assignments for similar complexes of cobalt(III) [8], the pair of resonances at δ −11.8 and −8.7 ppm is assigned to the carbon atoms adjacent to the secondary amine, the second pair at δ −27.9 and −27.5 ppm is assigned to the carbon atoms adjacent to the thiaethers, and resonances at δ −29.5 and −12.8 ppm are assigned to quaternary carbon atoms The resonance at δ −37.4 is assigned to the methyl carbon. The seven lines observed in the spectrum are consistent with the sample being diamagnetic in solution, the metal ion being bound symmetrically within the cavity of the encapsulating ligand with the expected C_3 symmetry. The ion has the metal and the three sulfur centers as chiral elements and

the ^{13}C NMR implies that the three thiaether centers have the same chirality and that on average all the chelate conformations of the three strands of the ligands are identical in solution. The ^{1}H NMR spectrum of the complex showed no indication of paramagnetic broadening at high temperature (345 K) at both pH 0.5 and 9.7 suggesting that the system is not near the spin crossover.

A positive-ion electrospray mass spectrum of $[Fe(AMN_3S_3sarH)](ClO_4)_3$ was recorded (Fig. 2). Little fragmentation of the molecular ion was observed, attributed to the high thermodynamic and kinetic stability of the complex [13]. The major ions detected occur at *m/z* 519 and 419 and are attributable to the ion pair ($[Fe(AMN_3S_3sar)]^{2+} + ClO_4^-$) and loss of a proton from the parent ion ($[Fe(AMN_3S_3sar)]^{2+} - H^+$), respectively. A relatively weak peak at *m/z* 210 can be assigned to the doubly charged ion $[Fe(AMN_3S_3sar)]^{2+}$. For the hexaamine cage complexes, including sarcophagine derivatives and expanded cage cavities, the doubly charged parent ion $[ML]^{2+}$ was always the most abundant ion observed (relative abundance 100%) whereas the deprotonated parent ion ($[ML]^{2+} - H^+$) if observed at all had a very low abundance (relative abundance < 5%) [13].

The structure of $[Fe(AMN_3S_3sarH)](ClO_4)_3 \cdot 3H_2O$ consists of the complex cation, three perchlorate anions and three water molecules. The terminal amine nitrogen on the encapsulating ligand is protonated, the protonation constant (log K_{HL}) being 4.9(1). The conformation of the complex cation is described as *lel*$_3$ since the C–C vectors of the N–C–C–S chelate rings are parallel to the C_3 axis of the complex [14]. The Fe(II)–N interactions (2.033(3), 2.048(3) and 2.049(3) Å) are similar to those reported for the low-spin iron(II) complexes $[Fe([9]aneN_3)_2]Cl_2$ (mean 2.03(1) Å) [15] and $[Fe([9]aneNS_2)_2](ClO_4)_2$ (2.038(4) Å) [4] but shorter than those reported for the high-spin octahedral complex $[Fe([9]aneN_2S)_2](ClO_4)_2$ (2.072(2) and 2.063(7) Å) [4]. The Fe(II)–S bond distances (2.226(1), 2.219(1) and 2.228(1) Å) are at the short end of the range reported for low- spin Fe(II)–S(thiaether) bonds. Amongst the shortest such bonds is that reported for the complex $[Fe(C_5H_5)(10S3)]PF_6$ (10S3 = 1,4,7-trithiacyclodecane) with 2.1823(7) Å [16] whilst other typical bonds lengths are those observed for the low-spin Fe(II) complexes of [9]aneS$_3$ (2.251(1), 2.241(1), and 2.259(1) Å) [3], [9]aneNS$_2$ (2.249(1) and 2.248(1) Å) [4], [18]aneN$_2$S$_4$ (1,4,10,13-tetrathia-7,16-diazacyclooctadecane) (2.2674 (15), 2.2673(16), 2.2578(17), 2.2588(16) Å) [17] and [18]aneS$_6$ (2.257_{av} Å) ([20]aneS$_6$ = 1,4,7,11,14,17- hexathiacycloeicosane) [18].

The electronic spectrum of $[Fe(AMN_3S_3sarH)]^{3+}$, in solution, appears typical of octahedral low-spin iron(II)

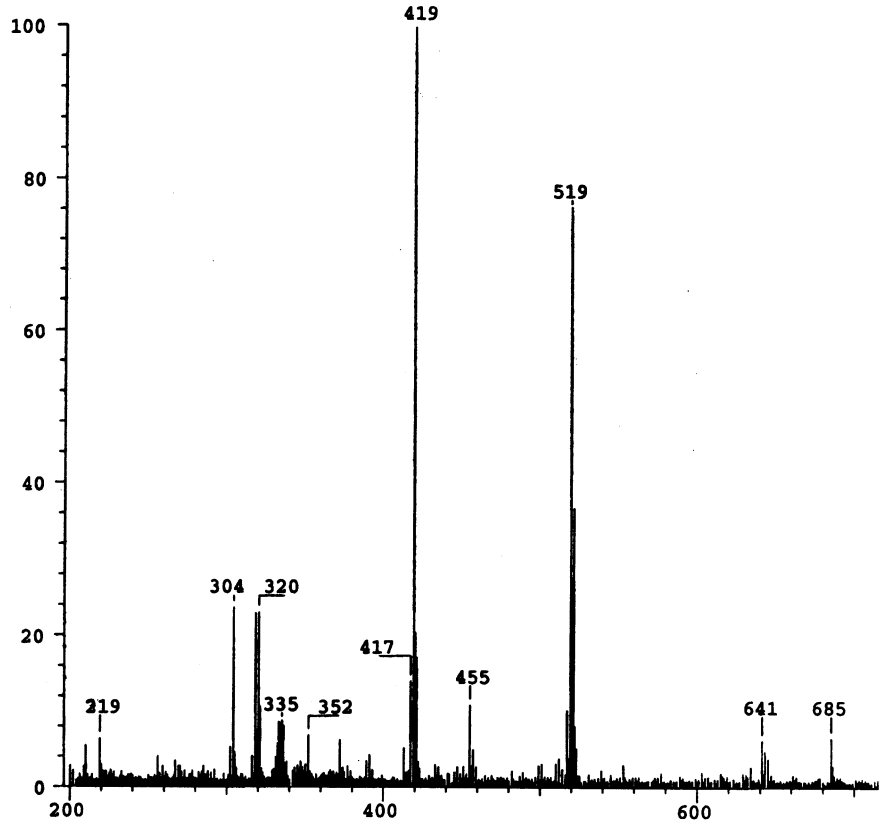

Fig. 2. Positive-ion electrospray mass spectrum of $[Fe(AMN_3S_3sarH)](ClO_4)_3$.

Table 3

Complex (coordination)	$^1A_{1g} \rightarrow {}^1T_{1g}$	$^1A_{1g} \rightarrow {}^1T_{2g}$	$10Dq^{LS}$, B (cm^{-1}) [a]	$10Dq^{LS}$, B (cm^{-1}) [b]	$10Dq^{HS}$	$\beta (= B/B_o)$ [c]	
$[Fe(ptz)_6]^{2+}$ (N_6)	549	379	20 550, 638 [d]		11 760	0.6	[2,26]
$[Fe([9]aneN_3)_2]^{2+}$ (N_6)	595	390	16 740, 738	17 130, 703	11 100	0.70 [a], 0.6 [b]	[15,36]
$[Fe(NH_2)sar]^{2+}$ (N_6)	590	394	17 160, 677	17 450, 656	11 000	0.64, 0.62	[5–7]
[Fe(*trans*-diammac)]$^{2+}$ [e] (N_6)	584	405	17 900, 578	17 840, 568		0.54, 0.53	[35]
$[Fe([9]ancN_2S)_2]^{2+}$ (N_4S_2)	581	406	18 070, 562	17 960, 553	9500	0.53, 0.52	[4]
$[Fe(Me_3[9]aneN_3)(MeCN)_3]^{2+}$ (N_6)	560	389	18 690, 598	18 610, 588	11 360	0.56, 0.55	[30]
$[Fe(AMN_3S_3sar)]^{2+}$ (N_3S_3)	559	404	18 980, 504	18 740, 499		0.47, 0.47	
$[Fe[9]aneNS_2)_2]^{2+}$ (N_2S_4)	551	412	19 350, 439	19 030, 434		0.41, 0.41	[4]
meso-$[Fe(10S3)_2]^{2+}$ (S_6)	550	399	19 310, 504	19 050, 498		0.47, 0.47	[18]
$[Fe[9]aneS_3)_2]^{2+}$ (S_6)	523	395	20 390, 440	20 050, 437		0.41, 0.41	[3,37,38]

[a] Calculated [27] assuming $C = 6B$.
[b] Calculated [27] assuming $C = 4B$.
[c] Bo (free ion), Fe(II) = 1060 cm^{-1} [34].
[d] ref [2] diammac = 6,13-diammino-6,13-dimethyl-1,4,8,11-tetraazatetradecane.

with two d–d bands at 559 and 404 nm [19]. Low-spin d^6 iron(II) complexes would be expected to exhibit two spin-allowed d–d transitions, $^1A_{1g} \rightarrow {}^1T_{1g}$ and $^1A_{1g} \rightarrow {}^1T_{2g}$. The visible spectrum was invariant with change in pH and there was no indication of the presence of a contribution from a high-spin iron(II) form of the complex nor of the presence of absorption bands corresponding to a coordinated imine. Spectra run as Nafion films at low temperature (10 K) did not exhibit spin-forbidden transitions ($^1A_{1g} \rightarrow {}^3T_{1g}$ and $^1A_{1g} \rightarrow {}^3T_{2g}$) [19].

In the absence of complete d^6 ligand field calculations it is possible to approximate the transition energies associated with the $^1T_{1g}$ and $^1T_{2g}$ excited states by the following diagonal energy expressions in order to evaluate the ligand field parameters, B, C and Dq [19–21]:

$$E(^1A_{1g} \rightarrow {}^1T_{1g}) = 10Dq - C$$

$$E(^1A_{1g} \rightarrow {}^1T_{2g}) = 10Dq - C + 16B$$

A better approximation for the spin-allowed transition energies are the following perturbation expressions, corrected for configuration interaction [22]:

$$E(^1A_{1g} \rightarrow {}^1T_{2g}) = 10Dq - C + (5BC + 7B^2 + C^2)/5Dq$$

$$E(^1A_{1g} \rightarrow {}^1T_{2g}) = 10Dq - C + 16B + (3BC - 27B^2 + C^2)/5Dq \quad (1)$$

In the absence of the spin-forbidden bands an approximation for C is required. For iron(II) complexes (d^6 low-spin) the approximation $C = 4B$ has been made and configuration interaction ignored [4,19–21], or included [23]. For cobalt(III) systems the assumption that $C = 6B$ has been applied on a number of occasions and configuration interaction also taken into account [22,24,25].

The iron(II) complex $[Fe(ptz)_6](BF_4)_2$ presents an opportunity to analyze a low-spin d^6 system in which both the spin-allowed and spin-forbidden bands have been observed, therefore, permitting a complete ligand field analysis. $[Fe(ptz)_6](BF_4)_2$ exhibits a light induced low-spin to high-spin conversion below 50 K [2,26]. The low-spin form exhibited spin-allowed transitions ($^1A_{1g} \rightarrow {}^1T_{1g}$; $^1A_{1g} \rightarrow {}^1T_{2g}$) at 549 nm and 379 nm, respectively. Additionally the spin-forbidden transitions $^1A_{1g} \rightarrow {}^3T_{1g}$ and $^1A_{1g} \rightarrow {}^3T_{2g}$ at 670 and 980 nm, respectively, were also identified. For this system it is reported that $10Dq = 20\,550$ cm^{-1} with $B = 638$ cm^{-1} and $C = 3742$ cm^{-1}, suggesting that $C = 6B$ is a better approximation for iron(II) systems, similar to the situation for cobalt(III) systems.

Therefore, assuming $C = 6B$ the spectral data for a series of low-spin iron(II) complexes can be examined. The series of complexes chosen (Table 3) represents a number of characterized low-spin iron(II) complexes for which the spectroscopic properties of the low-spin form have been reported. The ligand field parameters for each complex, setting $C = 6B$ in equations (1), have been determined [27] (the ligand field parameters for $C = 4B$ have also been included for comparison). Obviously the magnitude of $10Dq^{LS}$ increases from N_6 to N_3S_3 to S_6 coordination. For iron(II) complexes with nitrogen donors it is suggested that for $10Dq^{LS} < 11\,000$ cm^{-1} the complex should be high-spin, spin crossover complexes should lie in the range $10Dq^{HS} \sim 11\,500$–$12\,500$ cm^{-1} and $10Dq^{LS} \sim 19\,000$–$21\,000$ cm^{-1} and with low-spin complexes $10Dq^{LS} > 21\,500$ cm^{-1} [28]. Gütlich et al. have suggested that because the change in bond lengths during the spin transition is not taken into account, the argument that the difference between the average spin pairing energy and 10Dq must be of the same order as thermal energies for spin crossover complexes is too simple a notion to be correct [28]. With this in mind, spin pairing energy is not considered in this analysis. Gütlich, and others, note that for iron(II) complexes with nitrogen donors the ligand field strength decreases from $10Dq^{LS}$ to $10Dq^{HS}$ by a factor

of approximately 1.74 for the thermal spin transition but that the average spin pairing energy changes by about the same order as the nephelauxetic effect [28,29]. For $[Fe([9]aneN_3)_2]^{2+}$, $[Fe([9]aneN_2S)_2]^{2+}$, $[Fe(Me_3[9]aneN_3)(MeCN)_3]^{2+}$ [30], $[Fe(ptz)_6]^{2+}$ and $[Fe(NH_2)_2sar]^{2+}$ the position of the $^5T_{2g} \rightarrow {}^5E_g$ transition has been reported and permits an assessment of $10Dq^{HS}$ (9500–11 000 cm^{-1}) for these complexes. The criteria for spin crossover complexes ($10Dq^{HS} \sim 11\,500$–$12\,500$ cm^{-1} and $10Dq^{LS} \sim 19\,000$–$21\,000$ cm^{-1}) are satisfied for $[Fe(ptz)_6]^{2+}$ ($10Dq^{LS}$ 20 550 cm^{-1}; $10Dq^{HS} = 11\,760$ cm^{-1}), $10Dq^{LS}$ is at the low end of the range for the systems where both high and low-spin forms are observed ($[Fe([9]aneN_3)_2]^{2+}$, $[Fe([9]aneN_2S)_2]^{2+}$, $[Fe(Me_3[9]aneN_3)(MeCN)_3]^{2+}$, $[Fe([9]aneN_2S)_2]^{2+}$ and $[Fe(NH_2)_2sar]^{2+}$). $10Dq^{LS}$ for *meso*-$[Fe(10S3)_2]^{2+}$, $[Fe([9]aneNS_2)_2]^{2+}$, $[Fe([9]aneS_3)_2]^{2+}$ and $[Fe(AMN_3S_3sar)]^{2+}$ appears to be at the lower limit of the range predicted for exclusively low-spin complexes [28].

It is apparent that the magnitude of 10 Dq is not the sole determinant of the spin state. It is well established that the thiaether donor has π-acceptor properties and the effect of this may be gauged by the decrease in the magnitude of B, and the nephelauxetic parameter β ($= B_{complex}/B_{free\ ion}$), from $[Fe([9]aneN_3)_2]^{2+}$ to $[Fe([9]aneS_3)_2]^{2+}$ reflecting the increasing covalent contributions of the iron(II)–thiaether bonds (Table 3). The progression from an N_4S_2 (in $[Fe([9]aneN_2S)_2]^{2+}$; $B =$ 562 cm^{-1}) to N_3S_3 (in $[Fe(AMN_3S_3sar)]^{2+}$; $B = 504$ cm^{-1}) donor set and the subsequent reduction in the magnitude of B reflects the effect of replacement of the secondary nitrogen by the more covalent Fe(II)–thiaether interactions. The same trends in B are seen whether the C/B ratio employed is 4 or 6 suggesting that the ratio only has a marginal effect on the magnitudes of the ligand field parameters [24,31–33]. The values of β for *meso*-$[Fe(10S3)_2]^{2+}$, $[Fe(AMN_3S_3sarH)]^{3+}$ and $[Fe([9]aneS_3)_2]^{2+}$ (0.47, 0.47 and 0.42, respectively) can be compared with that reported for $[Fe(CN)_6]^{4-}$ (0.49) where the metal–ligand bond also has a large degree of π-acceptor character [19].

4. Conclusion

For the $[Fe(AMN_3S_3sarH)]^{3+}$ complex, the magnetic behavior is not influenced by pH or temperature, suggesting that this complex is also rigorously low-spin. The short Fe(II)–S(thiaether) bonds, amongst the shortest reported, are indicative of a large degree of metal–ligand orbital mixing (π-acceptor character) of the thiaether ligand, and this is reflected by the magnitude of the spectroscopic parameters 10 Dq and particularly B. These effects contribute to stabilizing the low-spin t_{2g}^6 condition for this complex.

5. Supplementary data

Crystallographic data are available from the The Director, CCDC, 12 Union Road, Cambridge, CB2 1EZ, UK (fax: +44-1233-336033; e-mail: deposit@ccdc.cam.ac.uk or www: http://www.ccdc.cam.ac.uk) quoting the deposition number CCDC No. 187142.

References

[1] H. Toftlund, Coord. Chem. Rev. 94 (1989) 67.
[2] A. Hauser, J. Chem. Phys. 94 (1991) 2741.
[3] K. Wieghardt, H.-J. Küppers, J. Weiss, Inorg. Chem. 24 (1985) 3067.
[4] V.A. Grillo, L.R. Gahan, G.R. Hanson, R. Stranger, T.W. Hambley, K.S. Murray, B. Moubaraki, J.D. Cashion, J. Chem. Soc., Dalton Trans. (1998) 2341.
[5] L.L. Martin, R.L. Martin, K.S. Murray, A.M. Sargeson, Inorg. Chem. 29 (1990) 1387.
[6] L.L. Martin, R.L. Martin, A.M. Sargeson, Polyhedron 13 (1994) 1969.
[7] L.L. Martin, K.S. Hagen, A. Hauser, R.L. Martin, A.M. Sargeson, J. Chem. Soc., Chem. Commun. (1988) 1313.
[8] L.R. Gahan, T.W. Hambley, A.M. Sargeson, M.R. Snow, Inorg. Chem. 21 (1982) 2699.
[9] G.M. Sheldrick, Acta Crystallogr., Sect. A 46 (1990) 467.
[10] G.M. Sheldrick, SHELXL-93, A Program for Crystal Structure Determination, University of Göttingen, 1993.
[11] C.K. Johnson, ORTEP, A Thermal Ellipsoid Plotting Program, Oak Ridge National Laboratory, Oak Ridge, TN, 1965.
[12] P. Gans, A. Sabatini, A. Vacca, J. Chem. Soc., Dalton Trans. (1985) 1195.
[13] S.F. Ralph, M.M. Sheil, L.A. Hick, R.J. Geue, A.M. Sargeson, J. Chem. Soc., Dalton Trans. (1996) 4417.
[14] *lel* and *ob* refer to limiting conformations of five membered chelate rings in which the $C-C$ axis is, respectively, parallel and oblique to the pseudo C_3 axis of the complex cation. See Inorg. Chem. 9 (1970) 1.
[15] J.C.A. Boeyens, A.G.S. Forbes, R.D. Hancock, K. Wieghardt, Inorg. Chem. 24 (1985) 2926.
[16] G.J. Grant, T. Salupo-Bryant, L.A. Holt, D.Y. Morrissey, M.J. Gray, J.D. Zubkowski, E.J. Valente, L.F. Mehne, J. Organomet. Chem. 587 (1999) 207.
[17] N. Atkinson, A.J. Lavery, A.J. Blake, G. Reid, M. Schröder, Polyhedron 9 (1990) 2641.
[18] G.J. Grant, S.M. Isaac, W.N. Setzer, D.G. VanDerveer, Inorg. Chem. 32 (1993) 4284.
[19] A.B.P. Lever, Inorganic Electronic Spectroscopy, 2nd ed, Elsevier, New York, 1984.
[20] D.A. Johnson, A.G. Sharpe, J. Chem. Soc. A (1966) 798.
[21] R. Dingle, C.J. Ballhausen, Mat. Fys. Medd. Dan. Vid. Selsk. 35 (1967) 1.
[22] T.M. Donlevy, L.R. Gahan, T.W. Hambley, R. Stranger, Inorg. Chem. 31 (1992) 4376.
[23] W.N. Setzer, E.L. Cacioppo, Q. Guo, G.J. Grant, D.D. Kim, J.L. Hubbard, D.G. VanDerveer, Inorg. Chem. 29 (1990) 2672.
[24] P. Osvath, A.M. Sargeson, A. McAuley, R.E. Mendelez, S. Subramanian, M.J. Zaworotko, L. Broge, Inorg. Chem. 38 (1999) 3634.
[25] R.A. Wentworth, T.S. Piper, Inorg. Chem. 4 (1965) 709.
[26] J. Jeftic, R. Hinek, S.C. Capelli, A. Hauser, Inorg. Chem. 36 (1997) 3080.

[27] adapted from L.C. Nathan, A Laboratory Project in Coordination Chemistry, Brooks/Cole Publishing Co., Monterey, CA, 1981.
[28] P. Gütlich, A. Hauser, H. Spiering, Angew. Chem., Int. Ed. Engl. 33 (1994) 2024.
[29] H.L. Schläfer, G. Gliemann, Einführung in die Ligandenfeldt, Akademische Verlagsgesellschaft, Wiesbaden, 1980, p. 462.
[30] D.W. Blakesley, S.C. Payne, K.S. Hagen, Inorg. Chem. 39 (2000) 1979.
[31] A. McAuley, S. Subramanian, Inorg. Chem. 29 (1990) 2830.
[32] T.M. Donlevy, L.R. Gahan, T.W. Hambley, K.L. McMahon, R. Stranger, Aust. J. Chem. 46 (1993) 1799.
[33] J.I. Bruce, L.R. Gahan, T.W. Hambley, R. Stranger, Inorg. Chem. 32 (1993) 5997.
[34] B.N. Figgis, Introduction to Ligand Fields, Wiley Interscience, New York, 1966.
[35] H. Börzel, P. Comba, H. Pritzkow, A.F. Sickmüller, Inorg. Chem. 37 (1998) 3853.
[36] J.W. Turner, F.A. Schultz, Inorg. Chem. 40 (2001) 5296.
[37] H. Doine, T.W. Swaddle, Can. J. Chem. 68 (1990) 2228.
[38] H.-J. Küppers, K. Wieghardt, B. Nuber, J. Weiss, E. Bill, A.X. Trautwein, Inorg. Chem. 26 (1987) 3762.